PCCP

Alumina/Clay Nanoscale Hybrid Filler Assembling in Cross linked Polyethylene Based Nanocomposites: Mechanics and Thermal Properties

Journal:	*Physical Chemistry Chemical Physics*
Manuscript ID:	CP-ART-04-2014-001532.R1
Article Type:	Paper
Date Submitted by the Author:	06-May-2014
Complete List of Authors:	Jose, Josmin; Mahatma Gandhi University, School of Chemical Sciences Thomas, Sabu; mahatmagandhi university, School of Chemical Science

Alumina/Clay Nanoscale Hybrid Filler Assembling in Cross linked Polyethylene Based Nanocomposites: Mechanics and Thermal Properties

Josmin P. Jose[1 a], Sabu Thomas[1, 2 b]

[1] School of Chemical Sciences, Mahatma Gandhi University, Kottayam, Kerala, India, 686 560

[2] International and Interuniversity Centre for Nanoscience and Nanotechnology, Mahatma Gandhi University, Kottayam, Kerala, India, 686 560

[a] josminroselite@gmail.com, [b] sabupolymer@yahoo.com

Abstract

Herein, investigation on XLPE/Al_2O_3/ clay ternary hybrid systems of Al_2O_3 and clay in 1:1 and 2:1 ratios, binary systems of XLPE/clay and XLPE/Al_2O_3 nanocomposites, with special reference to the hybrid filler effect and the superior micro structural development in ternary systems is conducted. Ternary hybrid composite of Al_2O_3 and clay in 1:1 exhibits highest tensile strength (100 % increase) and Young's modulus (208 % increase), followed by Al_2O_3: clay=2:1 system. The interaction between alumina and clay altered the composite morphology, filler dispersion and gave rise to a unique filler architecture leading to substantial boost up in mechanics compared to predictions based on idealized filler morphology. Experimentally observed much higher mechanics compared to theoretical predictions confirmed that, the dramatic improvement in mechanics is the outcome of positive hybrid effect and a second factor of synergism *i.e.* filler/filler networks. Morphological control of hybrid filler network is realized by adjusting ratio between different fillers. For Al_2O_3: clay = 2:1 system, the micro structural limitation of dispersion due to the steric effect of alumina clusters, shift the properties to the negative hybrid effect region.

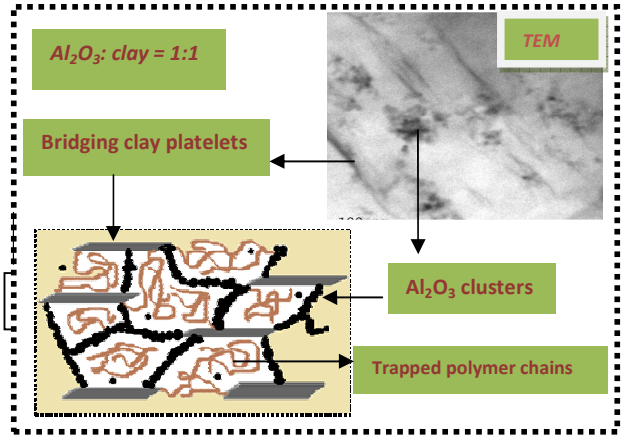

Key words: Hybrid fillers, synergistic effect, hybrid effect, mechanics, filler networks, cross-linked polyethylene

1. Introduction

Recent and ongoing research on organic/inorganic polymer nanocomposites has shown significant improvements in mechanical and thermal properties, without compromising on other properties and processability. The major challenge faced by these nanocomposites is the incompatibility between the organic polymer and inorganic filler and as a result, there exist a strong tendency of aggregation of nanoparticles.[1,2] Surface treatment on nanoparticles can reduce the degree of aggregation to some extent by two ways: (i) by reducing the surface free energy of nanoparticles, (ii) by increasing the compatibility between the polymer and inorganic oxide nanofillers.[3] Even the surface treatment has not fully succeeded in avoiding the strong aggregation tendency of nanoparticles and thus their negative effect on properties at higher filler loadings due to the dominant filler-filler interaction over filler-matrix interaction. Very recently, hybrid ternary systems, having two nano scale materials have found very promising in enhancing the dispersion of nanoparticles.[4,5] The super microstructure development associated with the synergism between the nano fillers leads to increased mechanical and thermal characteristics.[6,7]

Two different filler types are often used in the case of three-component compounding, which produces so called hybrid structures, in which, properties of different components are combined.[6] Hybridisation with more than one filler type in the same matrix provides another dimension to the potential versatility to the parent system. Properties of the hybrid composite may not follow a direct consideration of the independent properties of the individual components. A positive or negative hybrid effect can be defined as a positive or negative deviation of a certain property from the rule of mixture behaviour.[8] Recent investigations on composites having multi component filler systems have focused mainly on thermoplastics and thermosets.[7] Superior mechanical and dynamic mechanical properties can be acquired by the synergistic effect of two filler types. Such synergistic interactions result in a unique micro structural development that ultimately influences the properties especially the mechanics of composites that contain both particles.[9] Depending on the shapes of the materials and the way they are combined, change in morphology and microstructure is expected. Additionally, the use of hybrid system is expected to improve the dispersion by eliminating the tendency of aggregation by the difference in surface characteristics of two kinds of nanoparticles.[10,11] Maldas *et al.* have studied hybrid fibre reinforced thermoplastic composites.[12] Morsy *et al.* have investigated hybrid effect of CNT and nano clay on physico-mechanical properties of cement mortar.[13] The results show that, the hybridisation could significantly affect the mechanical properties. Sue et al. analysed the preparation of epoxy hybrid composites based on CNT and clay.[14] Uddin *et al.* have reported that silica nanoparticles reduced the agglomeration of alumina nanoparticles in the epoxy matrix dispersed by sonication method.[15] Chen *et al.* have studied the enhancement in mechanical properties of epoxy/silica nanocomposites by introducing graphene oxide to the interface. Results showed that the incorporation of SiO_2−GO hybrid significantly improved composites' mechanical properties, the mechanical reinforcement efficacy of SiO_2− GO is far better than that of binary composites.[16]

Selection criteria for hybrid fillers mainly based on the dimensionality of the filler in nano level. Low dimensional fillers are more difficult to disperse than their three dimensional cousins. The difference arises, because three dimensional quasi spherical particles touch at a point, whereas two dimensional layered silicates have less contact area, that exists naturally as stacks.[17] At the same time, both the systems are not free from the problem of aggregation. The combination of two and three dimensional filler types may synergistically act one another and produce a system with more efficient dispersion. This selection criterion favours the hybridisation of spherical nanofiller and clay platelets.[18] As XLPE nanocomposites are major candidates for insulation cable application, the effective dispersion of nanofillers in XLPE by the hybridisation of nanofillers is very much significant in the present level of nanocomposites fabrication, lacking efficient nanofiller disribution. For dielectric applications inorganic oxides are the best candidates of nano reinforcement. From the previous studies on comparison of different inorganic oxides filled XLPE composites, it is found that, Alumina nanofiller is the most efficient one. So it tried have a better morphology by hybridising alumina and clay.

In the present paper, we report the fabrication of a completely new system of XLPE based Al_2O_3/clay hybrid nanocomposites and their mechanical, dynamic mechanical and thermal characteristics. Structure-property correlation is established by the estimation of the microstructure by physical and chemical network density and TEM analysis. The objective of the paper is to provide insight into the micro mechanics of ternary hybrid nanocomposites, by taking care of the so called hybrid effect of spherical Al_2O_3 and clay platelets, that involves the networking mechanism and the effective dispersion by eliminating the tendency of aggregation, as a whole its contribution towards ultimate property enhancement of XLPE system.

2. Experimental

2.1 Materials

Low density polyethylene (PETROTHENE NA951080), density 0.94 g/cm^3 was obtained from Equistar, United States. The cross linking agent dicumyl peroxide (DCP) and antioxidant Irganox were used. The nano Al_2O_3 with 100 % silane, trimethoxyoctyl-reaction product (average particle size 23 nm), nanoclay: Bis(hydrogenated Tallow Alkyl)dimethyl, ammonium salt with Bentonite were obtained from Evonik Industries, United States.

2.2 Nanocomposite Fabrication

XLPE/Al_2O_3 /clay hybrid ternary composites of Al_2O_3 and clay in 1:1 and 2:1 composition, binary composites of XLPE/Al_2O_3, XLPE/clay composites were prepared by melt mixing using dicumyl peroxide as the curing agent. The cross linking agent, DCP 1.5 wt% and antioxidant 0.5 wt% were used. The mixing was done in a Haake mixer at 160 ^{0}C and 60 rpm for 12 minutes. The temperature, rotation speed, time of mixing and the amount of DCP and Irganox were kept constant for all mixes. The mixed nanocomposites were compression molded in a SHP-30 model hydraulic press with a maximum pressure of 200 kg/cm^2 at 180

°C for 5 minutes. High pressure was applied while moulding, otherwise the escaped methane, the cross linking by-product will form pores in the films. For all nanocomposites, the nanofiller concentration was kept fixed as 5 wt% and clay/XLPE composite is designated as C, Al_2O_3/XLPE composite is designated as A, Al_2O_3:clay = 1:1 composite is designated as A1C and Al_2O_3:clay = 2:1 composite is designated as A2C. Composite of XLPE without nanofiller, designated as X was also prepared for comparison.

2.3 Nanocomposite Characterizations

2.3.1 Transmission Electron Microscopy (TEM)

The dispersion of nano fillers in polymer nanocomposites was investigated using TEM. The micrographs of the nanocomposites were taken in JEOL JEM transmission electron microscope with an accelerating voltage of 200 keV. Ultrathin sections of bulk specimens (about 100 nm thickness) were obtained at -120 ^{o} C using an ultra microtome fitted with a diamond knife.

2.3.2 X Ray Diffraction (XRD)

The state of clay in nanocomposites can be studied by X ray diffraction studies using a wide angle X-ray diffractometer (WAXD) with Ni filtered CuK∞ source having wavelength, λ=0.154 nm operated at 40 KV and 30 mA with a step size of 0.02 from 2 theta 1^0 to 10 ^{0}(D8 Advance, Bruker AXS, Germany).

2.3.3 Tensile Tests

Tensile tests were performed at room temperature using EOLEXOR 500 N/Auto sampler (ASSS) (GABO Qualimeter Testanlagen Gmbh) machine. The dumbbell shaped samples of thickness around 0.3 mm, with 10 mm length in between clamps were used. The span length and cross head speed used for the testing were 40mm and 50mm/min, respectively. Yield strength and young's modulus were calculated by plotting nominal stress vs nominal strain curve. The stress-strain behaviour of all the nanocomposites at 120 ^{o}C was also analysed to estimate the network density of the system from the modulus value. At 120 ^{o}C, the crystalline fraction melts, which is the main contributor of the modulus value of a semi crystalline polymer below its melting temperature. So at 120 ^{o}C, modulus value is the direct result of the network structure of the XLPE as a result of cross-linking and physical entanglements. This is the best way to avoid the contribution of cystallinity.

2.3.4 Swelling Studies

Circular samples (diameter ≈ 2 cm) of ASTM standard D5890 were weighed and immersed in toluene contained in test bottles with airtight stoppers kept at 100 ^{o}C temperature. Initial weight, swollen weight and deswollen weight were taken on a highly sensitive electronic balance. Cross-link densities of the samples were calculated from swellings experiments using Flory Rehner equation.

2.3.5 Dynamic Mechanical Analysis

Dynamic mechanical properties were analysed in shear mode using Home-made machine in MATEIS,INSA de Lyon, France. Rectangular samples at frequency 1 Hz, angle 10^{-2}, couple range 10^{-5} to 10^{-8} were tested. Temperature range of 100 K to 400 K at 1K/minute used for the experiment. Liquid N_2 atm is used to reduce the temperature to 100K. Storage modulus, and loss modulus were calculated using DMA.

2.3.6 Thermogravimetric Analysis (TGA)

The thermal stability and decomposition characteristics of nanocomposites were tested using Netisch TG209 F3 Tarsus at N_2 atmosphere. The heating rate was 10 ^{o}C/minutes from 25 ^{o} C to 800 ^{o}C. Decomposition temperature and the amount of residue were estimated from TGA.

3. Results and Discussion

3.1 Morphology of Nanocomposites

3.1.1 Transmission Electron Microscopy

Transmission Electron Microscopy images provided information about the state of dispersion of nanoparticles in the nanocomposites. A typical surface treated nanocomposite dispersion micrographs are shown in Figure 1. TEM observations indicate that, different composite structures are attained for different binary and ternary nanocomposites. XLPE/Al_2O_3 (Figure 1a) exhibits aggregation tendency of nano Al_2O_3 particles, while XLPE/clay composite (Figure 1b) shows nice intercalating structure of clay platelets in XLPE matrix. To understand the synergistic effect between nano Al_2O_3 and clay platelets, the morphology of the composites with different filler proportions of Al_2O_3 and clay in 2:1 (Figure 1c) and 1:1 (Figure 1d) rations were examined. It is noted that, the filler network are formed with the mixed fillers of Al_2O_3 and clay, demonstrates a complex microstructure of multiple clay bridging of adjacent alumina particles. This kind of effective networking occurs only in Al_2O_3:clay = 1:1. For Al_2O_3:clay = 2:1 system, alumina aggregation dominates over hybrid effect in network formation. Since the natural structure and proportions of the fillers in ternary system are different, the morphology displays diverse features. In mechanics, ternary system dominates over the binary system of single filler composites, and this is demonstrated by the networking, and effective alignment and a state of efficient dispersion attained by the synergism between the fillers.[6-10] It was shown that, when clay nanoplatelets were introduced into the nanocomposites, the gaps between the Al_2O_3 nanoparticles were effectively filled and they were linked together through clay platelets, resulting in the formation of networks.[19]The TEM image of the 1:1 hybrid composites is schematically interpreted in the abstract graphic. In Figure 2, TEM images of A1C at different resolutions are given to confirm the predominating effect of hybrid filler alignment, especially in Figure 3C, it can be seen very clearly the interacting Al_2O_3 particles and clay platelets, which is the root of the network designing in the hybrid system of 1:1 ratio. The vander Waal's interaction between the alkyl

part (R) of the surface treatment on alumina nanoparticle (-trimethoxyoctyl) and clay platelet (-Bis(hydrogenated Tallow Alkyl)dimethyl) may take part in the alignment of hybrid fillers and thereby effective network formation. This kind of interaction is schematically represented in Figure 3. In addition, the interaction between alumina and clay not only altered the composite morphology—filler dispersion—but also gave rise to a unique filler architecture.[20] As the surface energy and surface characteristics of both the fillers are different, aggregation tendency is minimized between these hybrid nanomaterials. For each combination of hybrid filler systems, there was an optimal volume ratio between the hybridising fillers. If the volume ratio of clay is too low, the limited number of fillers restricts the degree of bridging between alumina nanoparticles. Leung *et al.* have reported a similar system, in which the bridging capacity of Boron nitride platelets with MWCNT and there by the formation of a structured network is investigated.[21]

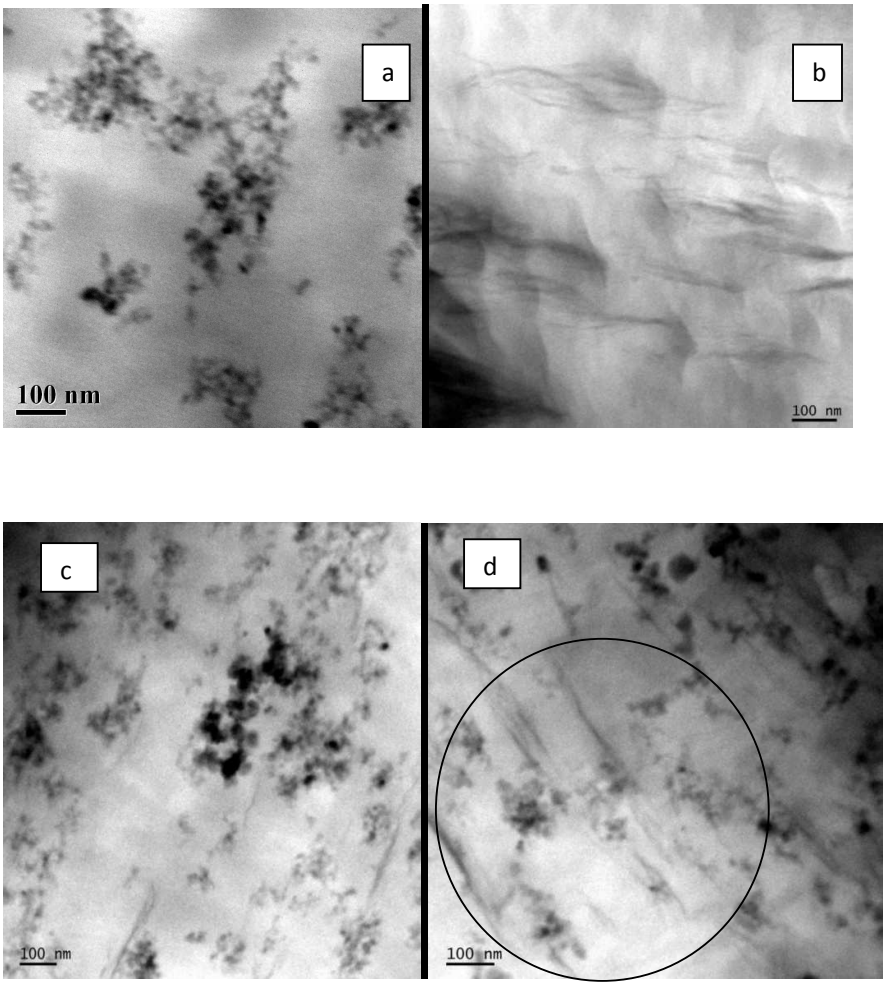

Figure 1 : Transmission electron micrographs of XLPE/Al_2O_3 (a), XLPE/clay (b), XLPE/ Al_2O_3:clay=2:1 (c), Al_2O_3:clay=1:1 (d)

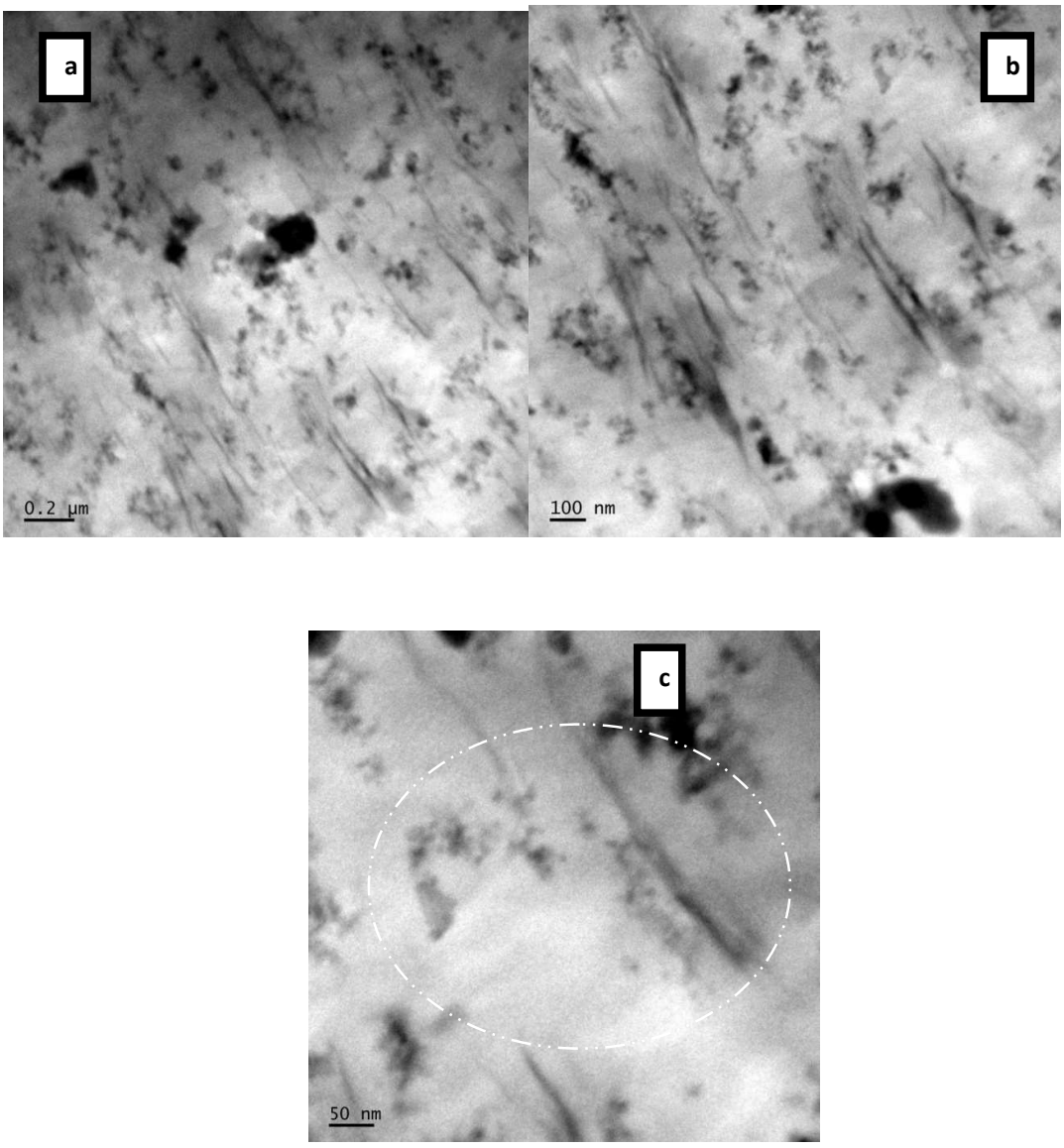

Figure 2 : Transmission electron micrographs of A1C at différent résolutions

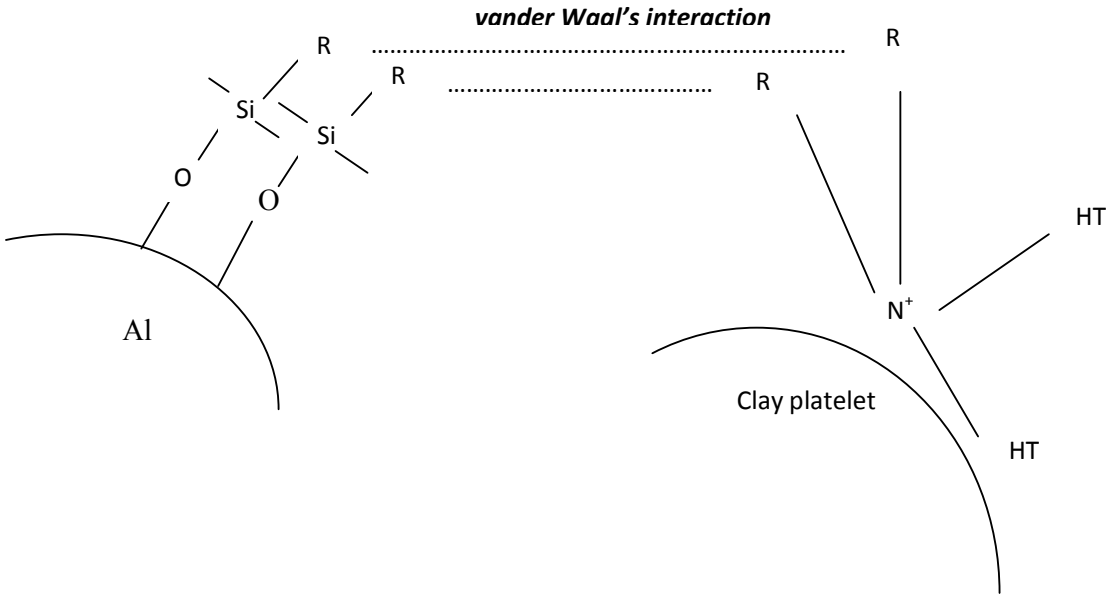

Figure 3: Schematic representation of interaction between silane, trimethoxyoctyl treated Al_2O_3 and Bis(hydrogenated Tallow Alkyl) dimethyl, ammonium modified nanoclay.

3.1.2 X Ray Diffraction

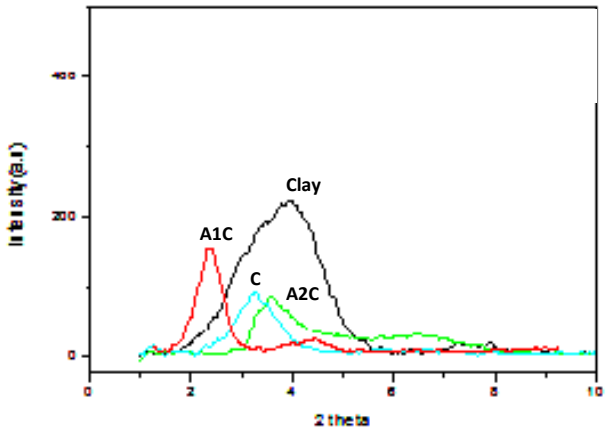

Figure 4: XRD patterns of nano clay, XLPE/clay (C), XLPE/ Al_2O_3:clay=1:1 (A1C), XLPE/ Al_2O_3:clay=2:1 (A2C)

The state of clay in nanocomposites can be studied by X-ray diffraction studies. The shift of (001) peak indicates the state of intercalation. There is association equilibrium between polymer and clay platelets during processing and a polymer can form bonds with another polymer or clay. WAXS data is shown in Figure 4. Pristin clay was found to have d_{001} = 22.50 nm, XLPE nanocomposites 26.9 nm (clay 5 wt%), 29.85 nm (alumina and clay in 1:1 ratio), and 26.15 nm (alumina and clay in 2: 1 ratio). The WAXS data show that, the peak value is significantly shifted to lower angles for the ternary hybrid composite of 1:1 ratio. The

presence of surface treatment on nano clay can lower the thermodynamic energy barrier for clay-polymer interaction, possibly allow a relatively higher number of polymer chains to migrate and stabilize within the clay platelet galleries and form a disordered intercalated system.[22] In the present system, XLPE/clay nanocomposite and XLPE/alumina clay 2:1 nanocomposite show the normal trend of intercalation. XLPE/alumina clay 1:1 nanocomposite exhibit highest d spacing with a sharp peak. Synergistic effect of nanomaterials promotes the intercalation in clay platelets and this system can maintain the ordered structure to some extent *i.e.* ordered intercalated morphology. Self aggregation of nano clay is reduced considerably by the synergism of hybrid materials and effective intercalation is possible. The sharp peak denotes the uniform morphology with equal d spacing everywhere, avoiding aggregation of particles and mixed morphology. Theoretical and experimental studies showed that, polymeric chains in the vicinity of flat surfaces tend to orient with their long axes parallel to the surfaces in order to minimize conformational distortions to the chains. The height of such an arrangement has been quantified as at least 0.4−0.7 nm, with the largest increases ascribed to a multiple layer assembly of the chains within the clay layers. On the basis of these data, it is reasonable to propose an increase in d spacing of 0.4 nm as a significant threshold that allows intercalation.[23] In our case, such increase is equal to almost 7.35 nm for hybrid system of 1:1 ratio, indicative of a very extensive insertion of the polymer chains in between the clay layers.

3.2 Mechanics

The tensile modulus (measure of stiffness) and yield strength (measure of onset of viscoelastic deformation) of materials are important selection parameters determinig final applications. Figure 5 shows the stress- strain behaviour of neat XLPE and nanocomposites. All the samples show a linear ealstic behaviour followed by an inelastic plastic deformation. It can be seen that, all the composites exhibit higher stress values than the unfilled systems over the entire range of strain. The tensile strength of the nanocomposites show higher values compared to the neat XLPE. The hybrid nanocomposite of Al_2O_3:clay = 1:1 shows highest yield strength. The presence of clay platelets reduces the aggregation tendency of alumina nanoparticles and due to the difference in surface characteristics between nanoparticles, it is dispersed properly.[24] Such synergistic interactions result a unique microstructural development which explains the very high increase in yield strength and Young's modulus value. Similar trends were observed by Konishi and Cakmak[25] for carbon black and clay system and which is attributed to the attraction between carbon black and clay that induces chaining of carbon black along the relatively large platelet face. An analogous concept has also been suggested for alumina nanomaterials in the presence of clay. The driving force behind the filler alignment is the interaction between the surface treatment on alumina nanoparticles and the organic modification on clay platelets.

Possible mechanism of this phenomenon can be discussed together with morphological observation. The altered microstructure is attributed to the interaction between alumina and clay in polymeric matrix, which results in synergistic stabilization of alumina and clay platelets, that involves the networking mechanism. The mechanism of micro structural

development as a function of alumina:clay ratio is speculated based upon the experimental results. Regarding the ternary systems containing both alumina and clay platelets, co-supporting networks are formed with two types of fillers. Bridging of alumina clusters through clay platelets occurs in Al_2O_3:clay = 1:1 nanocomposite. This is schematically represented in the abstract image. At low clay concentration (Al_2O_3:clay = 2:1 system), the distribution and the interaction is influenced by steric effect of alumina clusters. For this system, network is not being efficiently built up, as the alumina nano particle interaction dominates. This indicates that there is no effective synergistic effect in 2:1 system compared to 1:1 system of ternary composites. This altered microstructure suggests an interaction between alumina and clay, which is the reason for improved mechanical properties by the effective dispersion and distribution of nanomaterials in polymer. The filler network act as an efficient reinforcement in the parent system, which provides superior mechanics to the nanocomposites. In this case effective stress transfer occurs from the continuous phase to the dispersed phase and in the dispersed phase filler networks are strong enough to withstand. Composites containing equal amounts of alumina and clay showed significant improvements in tensile strength (100 % increases) and modulus (208 %) as compared to those containing an equivalent amount of only one type filler. Furthermore, synergistic interaction between clay and alumina can influence the dispersion state of alumina in XLPE matrix.[26-29] The tensile results correlates with the structure-property relationship, which is revealed by the TEM images. While comparing with the binary systems, XLPE/ Al_2O_3 nanocomposite is superior to the XLPE/clay nanocomposites. The key factors behind this are the effect of surface treatment on Al_2O_3 nanoparticle and the very large surface area of three dimensional nanofiller Al_2O_3. By the surface treatment on Al_2O_3, the nanoparticle suface becomes hydrophobic in nature (more organic and nonpolar character) and this will increase the compatibility with the matrix having similar surface properties.[30] Since XLPE and nano Al_2O_3 are purely organic/inoraganic system, both will be phase separated during the preaparation. But the presence of alkyl group on the Al_2O_3 nanoparticle act as a bridge between filler and polymer as the -OCH_3 part of trimethoxyoctyl silane will be chemically bonded to Al_2O_3 and the octyl part will form linkage with polymer and this leads to the enhanced interaction between polymer and filler. In the case of nanocomposites, the presence of surface treated Al_2O_3 strengthens the matrix, due to strong interfacial interaction between the components. A good interface will restrict the deformation of the polymer and leads to a higher tensile strength.[31]

Young's modulus values of XLPE and nanocomposites are given in Table 1. A significant increase in Young's modulus is observed for the Al_2O_3:clay = 1:1nanocomposite (208 % increase compared to neat XLPE). Modulus enhancement depends on intrinsic properties of matrix as well as interactions between matrix and filler. The reinforcing capability of nanofillers is caused by an immobilization of the polymer chains.[32] The very high modulus value is the direct result of reduction in mobility of polymer chains. The polymer filler interaction can contribute towards physical network density. For the hybrid composites, polymer chain immobilization could be attained by (1) trapping of polymer chains in the filler networks, (2) transformation of normal polymer chain to the constraint polymer in the vicinity of nanofillers.[33] The immobilized polymer layer(constraint polymer) around the filler

surface, is the direct result of the effective interaction between filler and polymer. This immobilized phase can contribute to the total network density of the polymer and thus the effective stress transfer in mechanical stretching.[34-36] It is understood that, an attractive interafce will decrease the mobility of the polymer chains and a repulsive interface will increase the mobility.[37] These results indicated that, the presence of the surface treatment on nanoparticle acts as a link between polymer matrix and inorganic particles and provides an attractive interface and this improved the interaction of these two phases and compatibility, resulting superior mechanical properties.[38] Further more, for the hybrid filler reinforced system of ternary composite, trapping effect contribute in addition to the immobilized phase, which explore the superior modulus value of the Al_2O_3: clay = 1:1nanocomposite compared to other nanocomposites.

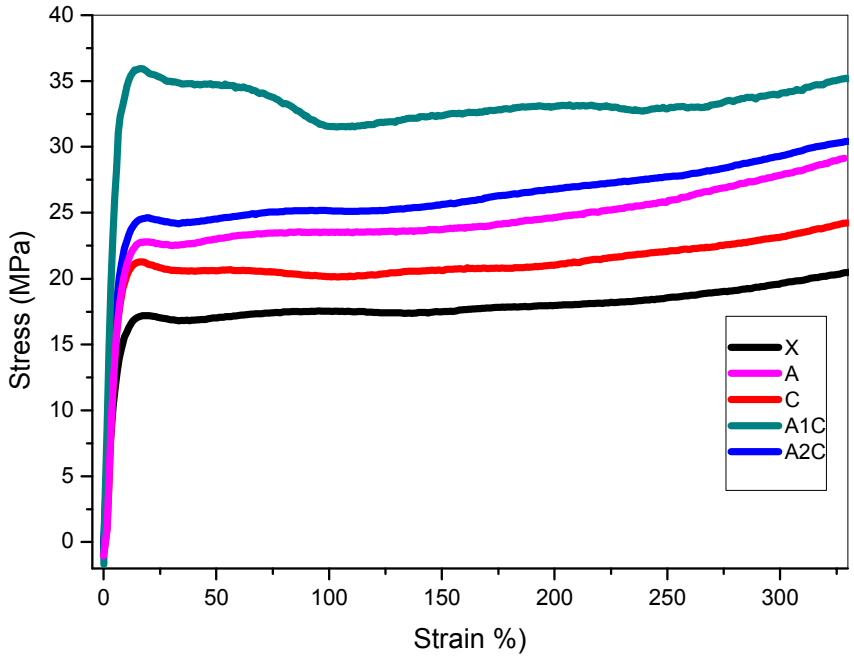

Figure 5: Stress-Strain behavior of XLPE (X), XLPE/ Al_2O_3 (A), XLPE/clay (C), XLPE/ Al_2O_3:clay=1:1 (A1C), XLPE/ Al_2O_3:clay=2:1 (A2C)

Sample	Young's modulus(MPa)
X	263 ± 10
C	370 ± 8
A	384 ± 6
A1C	812 ± 9
A2C	555 ± 11

Table 1: Young's modulus of XLPE (X), XLPE/ Al_2O_3 (A), XLPE/clay (C), XLPE/ Al_2O_3:clay=1:1 (A1C), XLPE/ Al_2O_3:clay=2:1 (A2C)

The explanation for very high modulus value is based on the assumption of special morphology of restricted mobility of polymer chains. During cooling from the processing temperature of the composite (180 ^oC) to room temperature, the filler particles are assumed to act as sites where thermal contraction is particularly favoured, which should cause the special morphology. When a semi crystalline thermoplastic is cooled down from the melt, a solidification process will take place. The thermal conductivity of the polymer is 0.1 – 0.2 $Wm^{-1}K^{-1}$ and that of ceramics is about 1-40 $Wm^{-1}K^{-1}$. Therefore it is assumed that the polymer adjacent to the embedded particles contract in an earlier stage of process, because of the difference in their thermal conductivities, a zone with a higher density (high modulus) will be formed around the particle. Owing to the heat transportation process, a depletion zone with relatively low density (low modulus) will be created surrounding the high density zone.

It is essentially due to the different thermal expansions of polymer (50 X 10^{-6} to 300 X $10^{-6}K^{-1}$) on one hand and ceramics (0.5 X 10^{-6} to 15 X $10^{-6}K^{-1}$) on the other hand.[33] According to Krevelan, Young's modulus E is proportional to the seventh power of density ρ

$E \alpha \rho^7$. This means that the starting zones, which have a higher density, have a higher Young's modulus and the depletion zones, which have a lower density, have a lower modulus. As the number of effective particles in polymeric matrix increases with proper dispersion, large quantity of high modulus region formation occurs, in accordance with.

The contributing factors to the improved mechanics of hybrid ternary nanocomposites can be summarized as (a) filler network formation, which leads to efficient reinforcement, (b) proper dispersion of nanofillers in XLPE matrix by evading the self aggregation tendency in the neighbourhood of another filler, leading to a uniform microstructure (c) formation of immobilized polymer phase in the vicinity of nano materials, (d) trapping of polymer chains inside the filler networks.

3.3 Network Density

Stress- strain behaviour at 120 ^{o}C of alumina and alumina/clay hybrid nanocomposites are given in Figure 6.

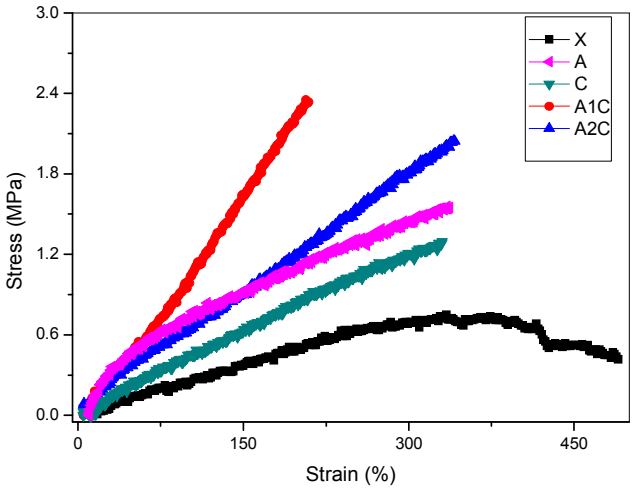

Figure 6: Stress-Strain behavior at 120 ^{o}C of XLPE (X), XLPE/ Al_2O_3 (A), XLPE/clay (C), XLPE/ Al_2O_3:clay=1:1 (A1C), XLPE/ Al_2O_3:clay=2:1 (A2C)

From the stress-strain behaviour, above the melting temperature, the modulus value could be attained. This modulus value will be the direct result of the network structure of the system, as the crystalline fraction melts at this temperature, which is the main contributor of the modulus value of a semi crystalline polymer below its melting temperature. Modulus value at 120 ^{o}C is shown in Table 2. Total network density is the sum of chemical cross links and physical networks. Nanoparticles can contribute towards both chemical cross links and physical networks by immobilized polymer fractions. The network density results confirm the role of hybrid fillers in network formation and there by trapping mechanism, as the modulus value is very high for Al_2O_3: clay = 1:1nanocomposite compared to other systems. The two ternary systems show higher values than the binary systems, which are superior to the neat polymer. This is due to the synergism between the fillers, which shows maximum efficiency at Al_2O_3:clay = 1:1. For a system of 2:1 ratio of hybrid fillers, due to the excess alumina concentration, self aggregation dominates over the interaction between alumina and clay platelets. This shows the network formation ability of A2C is less than that of A1C composite, but higher than that of binary composites of alumina or clay alone systems.

All the reinforced systems shows superior network density compared to the neat XLPE. For the binary system, the network density enhancement can be correlated to the formation of

constraint zone, while for the hybrid ternary system; it is the sum of the trapped polymer chains in the filler networks and the constraint zone.

The nanoparticle incorporation in a polymer creates interactions between the nanoparticles and the polymer chains, which are located in the nanoparticle vicinity. These interactions cause regions with restricted chain mobility around the nanoparticles. The immobilized polymer layer around the filler surface is the direct result of the effective interaction between filler and polymer. If the interaction between the filler and the amorphous phase is strong, a definite amount of constraint polymer fraction will generate.[34] Here the nanofiller surface is acting as an adsorption site and initiate the solidification process. First of all, the physical network junctions at the polymer-filler interface contribute to the total network density of the polymer.[38] Second, the polymer-filler interaction significantly increases the energy required to breakdown the nanoparticle aggregates during deformation. Finally, the physical junctions could dissipate energy during deformation, as a result of the chain slippage along the filler surface and breaking and reaggregation of filler clusters.[30]

The network structure in the matrix is largely affected by morphological and the molecular scale heterogeneity of filled system, *i.e*. (i) the chemical heterogeneity of unfilled system, (ii) the morphological heterogeneity of the filled systems due to the spatially heterogeneous distribution of the filler particles and their aggregation and agglomeration, (iii) the heterogeneous distribution of chemical cross-links in the system, (iv) the polymer-filler interface.[32] The following types of network junctions are present in XLPE hybrid nanocomposite systems: chemical cross-links and XLPE–alumina/clay physical adsorption junctions. The filler surface also could restrict chain motions due to the excluded volume effect of the filler particles. The structure of physical network consists of a dense physical network and an entangled loosely bound chain with hardly any adsorption junctions. In this rigid filler limit, the elastic energy is stored in the distorted strain field, around the particles.

According to Tanaka's multicore model of interface formation around a nanoparticle, when a spherical inorganic surface treated nanoparticle is embedded in a polymeric matrix, three layers are formed around it, as far as the chemical aspect is considered.[39] The bonded layer (first layer) is a transition region, which is tightly bonded to both nanoparticle and polymer by silane couplings. The thickness of the first layer is around 1 nm. The bound layer (second layer) consists of polymer chains strongly bound to the first layer. The thickness of this layer is between 2 nm and 9 nm. The chain mobility is characterized by this region. When curing agents are absorbed to nanoparticles, a layer of stoichiometrically cross linked thermoset with excess curing agent is formed around the nanoparticles. The loose layer (third region) is a region loosely coupled to the second region. It has different chain structure and mobility, free volume and crystallinity compared to the polymer. Its thickness is about several tens of nm. The role of second and third regions seems to be pivotal in order to explain various properties, whereas the first layer plays an indirect role. The schematic representation given in Figure 7 represents the polymer chain dynamics as a function of distance of polymer chains from the vicinity of nanofiller surface.

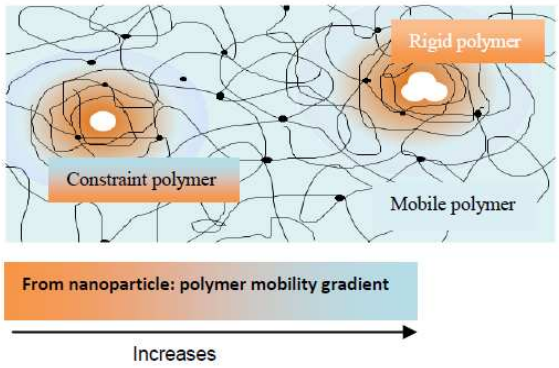

Figure 7: Schematic representation of polymer chain dynamics in nanocomposites

3.4 Crosslink Density

According to the theory of swelling of cross-linked polymers, strong bonds, such as the chemical cross links between the XLPE chains, prevent the molecules becoming completely surrounded by the fluids, but cause swelling. Cross link density is frequently calculated from equilibrium swelling data by means of the Flory-Rehner equation.[33,40-41] and this equation relating swelling behaviour to the kinetic theory through the polymer–solvent interaction parameter or Huggins factor.

Cross link density $V = 1 / 2M_c$ .....(1)

Where M_c is the molecular weight of polymer between cross-links

$M_c = [-\rho_r V_s V_{rf}^{1/3}] / [\ln (1-V_{rf}) + V_{rf} + \chi V_{rf}^2]$ ……..(2)

Where ρ_r is the density of polymer, V_s is the molar volume of solvent and V_{rf} is the volume fraction of the polymer in the swollen sample and is given by:

$V_{rf} = [(d\text{-}fw)/ \rho_r] / [(d\text{-}fw) / \rho_r) + (A_s/ \rho_s)]$ …… (3)

Where d is the deswollen weight, f is the volume fraction of the filler, w is the initial weight of the sample, ρ_r is the density of polymer, A_s is the amount of solvent absorbed. In equation (2), χ is the interaction parameter and is given by Hildebrand equation

$\chi = \beta + [V_s(\rho_s - \rho_p)^2 / RT]$ ……..... (4)

Where β is the lattice constant, R is the universal gas constant, T is the absolute temperature, ρ_s is the solubility parameter of solvent and ρ_p is the solubility parameter of polymer.

Sample	Cross-link density x 10^4 (mol/cm^3)	Modulus at 120 ^{o}C (MPa)
X	1.0	0.357
A	1.6	0.666
C	0.85	0.454
A1C	1.7	1.25
A2C	1.3	1.0

Table 2: Cross link density and modulus at 120 ^{o}C of neat XLPE and nanocomposites

Cross link density values obtained by swelling experiments are presented in Table 2. Nanocomposites exhibit higher values except clay nano composite. Silane coupling agents on alumina nanoparticle can act as network forming agents, which are able to react with the polymer chains leading to the formation of a cross linked network. The alkyl tail of silane surface treatment can take part in cross-linking with polymer chains through the same mechanism of radical initiation by the addition of peroxide. The physical networks of filler/matrix and filler/filler networks in hybrid systems also have major contribution towards the cross-link density of the composites. The XLPE/clay binary composites, the effect of filler on chain immobilization and thus the physical entanglements is less as it is a 2D nanofiller with less nanosurface. According to Barus *et al.* radicals on the polymer chains could easily react with vinyl groups of vinyl siane treated nanofillers and this could promote the cross link formation between matrix and filler.[42-43]

3.5 Hybrid Filler Effect

Hybrid reinforcing effect of the two nano fillers has been theoretically calculated. The law of additive rule of hybrid mixtures was used to calculate the hybrid effect. The rule is given by:

$$X_H = X_1V_1 + X_2V_2 \quad \text{.....(5)}$$

Where X_H , a characteristic property of the hybrid composite, X_1 and X_2 are characteristic properties of individual composites and V_1 and V_2 are the volume fractions of the reinforcement in hybrid composites.[44] Properties of hybrid effect follow a positive or negative hybrid effect, which may be independent of the properties of the individual properties.

Figure 8 shows schematically the fields occupied by two families of materials, plotted on a chart with properties P_1 and P_2 as axes. Within each field a single member of that family is identified (Materials M_1 and M_2).[45] The diagram shows that, what might be achieved by making a hybrid of two. There are four scenarios, each, typical of a different class of hybrid. Depending on the shapes of the materials and the way they are combined, there are four possibilities. The best is the point A where, positive hybrid effect is shown. These are examples for most commonly, when a bulk property of one material is combined with the surface properties on another. When the hybrid effect is the arithmetic average of the properties of components, weighed by their volume fractions, it is represented by Point B,

which obeys the rule of mixtures. The weaker link dominates in Point C, in which the hybrid properties fall below those of the rule of mixtures, lying closer to the harmonic than the arithmetic mean of the properties. Point D represents the worst of all scenarios.

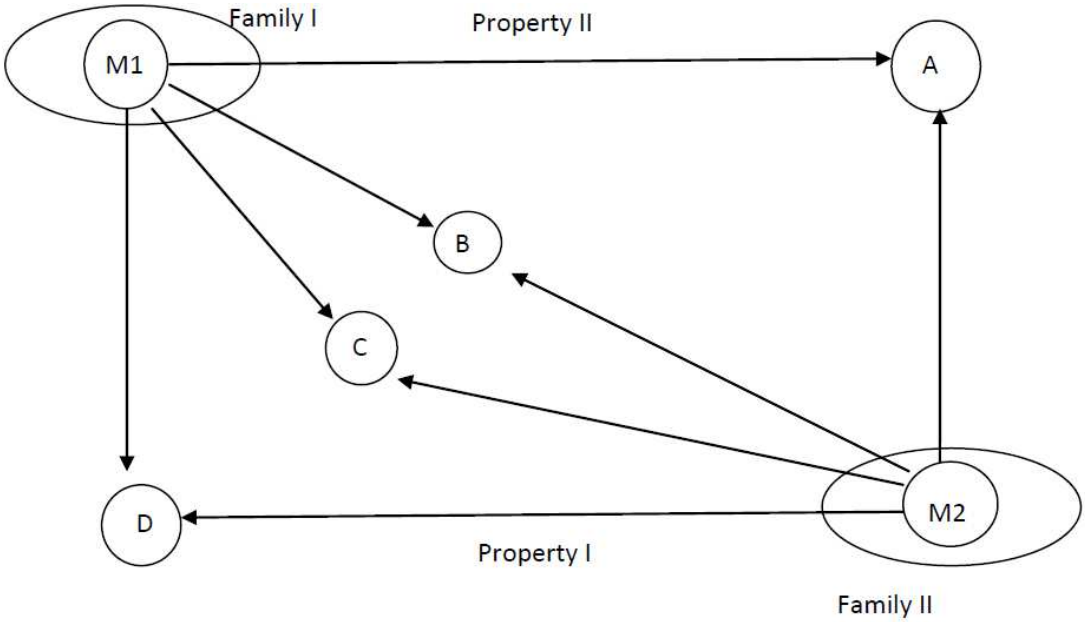

Figure 8: Schematic representation of properties of different hybrid combination

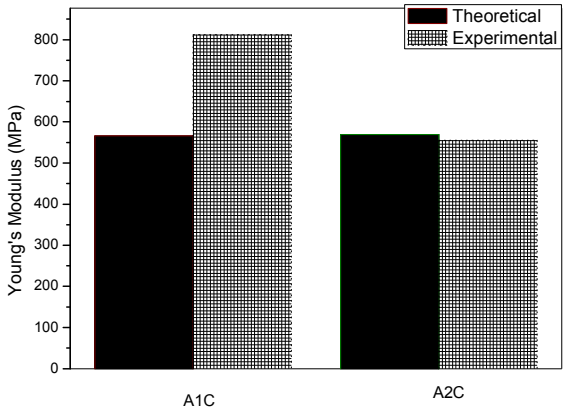

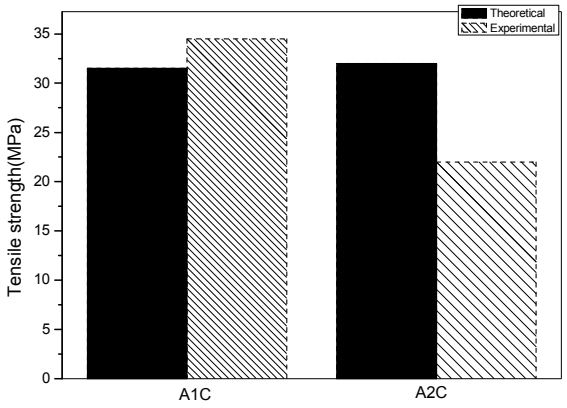

Figure 9: Comparison of theoretical and experimental values of Young's modulus and tensile strength of in Al_2O_3 : clay = 1:1 and in Al_2O_3 : clay = 2:1nanocomposites

Theoretical and experimental values of Young's modulus and tensile strength are compared in Figure 9. For the present system, Young's modulus and tensile strength of the hybrid composite Al_2O_3:clay = 1:1, experimental result shows positive hybrid effect, indicated by the point A, make clear that in addition to the arithmetic average, another factor also have significant role. In the hybrid system containing both alumina and clay platelets, co-supporting networks are formed with two types of fillers. Bridging of alumina clusters through clay platelets occurs in Al_2O_3:clay = 1:1nanocomposites. This microsructural development reveals the mechanics totally.

For the hybrid system of composite Al_2O_3:clay = 2:1, Young's modulus exhibit slight negative hybrid effect (can be represented by C), nevertheless tensile strength show a large negative hybrid effect (can be represented by D). For Al_2O_3:clay = 2:1 system, the micro structural limitation of dispersion due to the aggregation of alumina particles shift the properties to the negative hybrid effect region.

3.6 Dynamic Mechanical Analysis

Storage modulus as a function of temperature is shown in Figure 10.

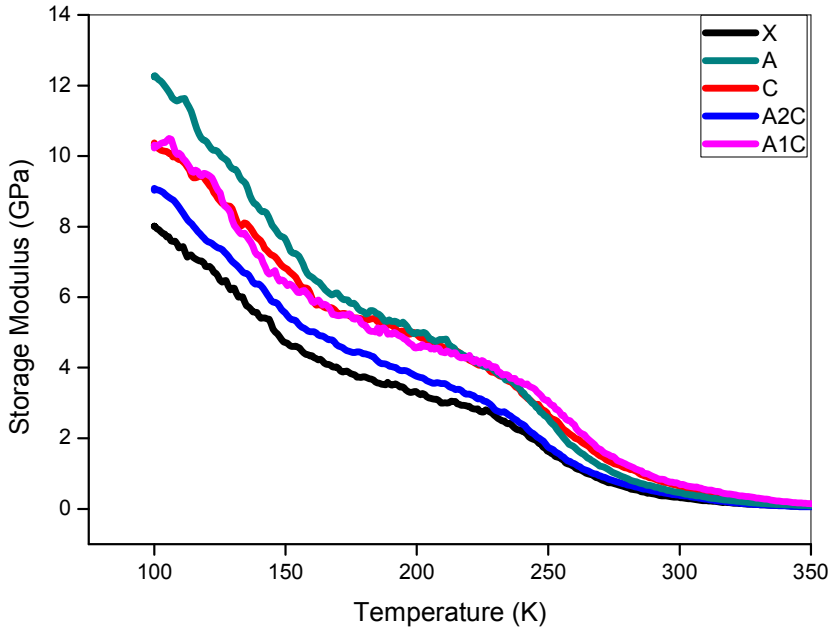

Figure 10: Storage modulus XLPE and nanocomposites as a function of temperature

As expected, the nanocomposites exhibit much higher storage modulus than pure XLPE, especially at low temperatures, given the reinforcing effect of nanoparticles. The storage modulus of the hybrid system is lower than that of XLPE/Al_2O_3 system at very low temperatures. When temperature is lower than –100 °C storage modulus decreases rapidly, and then it decreases gently at the temperature range lower than –50 °C. In a temperature range of –50 °C ~ 25 °C, storage modulus decreases quickly with a rise in temperatures, and then it decreases slightly. In other words, the turning points of storage modulus-temperature curves are at about –100 °C, 0 °C, and 80 °C, respectively.[46] With a rise of temperature, the motion ability of molecular chain in the resin enhances and the relaxation process of the elastic storage energy is quickened, resulting the reduction of the storage modulus.[47]

Sample	Storage modulus at 100 K(GPa)	Storage modulus at 300 K (GPa)	Coefficient ‘c’
X	8	0.3	-
A	12.2	0.5	0.76
C	10.4	0.6	0.65
A1C	10.4	0.7	0.55
A2C	9	0.4	0.84

Table 3: Storage modulus at 100 K, 300K and co-efficient ‘c’ of neat XLPE and nanocomposites

The effectiveness of fillers on moduli of the composites can be represented by co-efficient such as

$c = (E'_G/E'_R)$ Composite / (E'_G/E'_R) Resin ……(6)

Where E'_G and E'_R are the storage modulus values below glass transition and above glass transition respectively.[41]

The lower the value of the constant 'c', the higher the effectiveness of the filler. The measured E' values at 100 K and 300K were employed as E'_G and E'_R respectively. The values of c obtained for different composites are given in Table 3. The effectiveness of the filler is highest for Al_2O_3 : clay = 1:1. Maximum stress transfer between matrix and filler takes place for this composition. The superior properties obtained for tensile strength and Young's modulus can be correlated to this result.

Figure 11 shows the loss moduli as a function of temperature for the unfilled XLPE and the composites. The α, β, ɣ transitions could be identified in loss modulus vs temperature curve: γ at -120 ^oC - glass transition, β at 0 ^oC - side chain movement, α at 80 ^oC orientation motion in crystals.[48] A higher value of loss modulus is noted for the composites, except hybrid system of 1:1 ratio, compared to the neat XLPE, and this implies excessive heat generation within the polymeric composite system. Several aspects contribute to this anticipated heat generation. This increase in the loss modulus was considered to be an upshot of liberation of heat of friction at the particle–polymer interface. It has been postulated by Nielsen and Landrel that particle–particle interaction can also evolve frictional heat. The particle–particle contact can arise from agglomeration of fillers. Due to the proper dispersion of nanoparticles, free volume will be very less and so the freedom of chain movement is less in hybrid system A1C. Also the absence of large filler aggregates, minimize the heat generation by particle-particle interaction.

From the DMA analysis the following results can be summarized. (1) Nanocomposites are showing higher storage modulus compared to neat XLPE. This is due to the increased stiffness of the material by the incorporation of material with more elastic modulus (2) Except for A1C, all other nanocomposites, the loss factor is higher compared to the pristine XLPE and this implies excessive heat generation within the polymeric composite system.

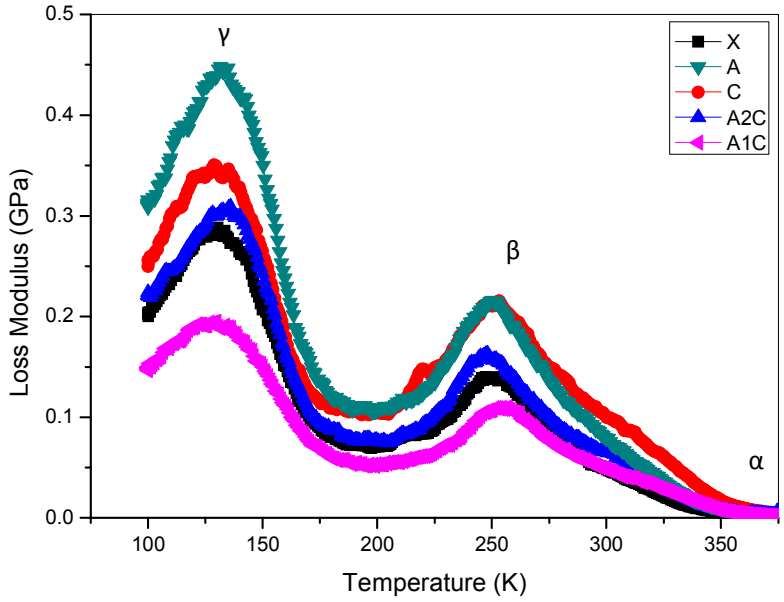

Figure 11: Loss modulus of XLPE and nanocomposites as a function of temperature

3.7 Thermogravimetric Analysis

Thermal degradation bahavior of nanocomposites has been investigated by employing TGA analysis in N_2 atmosphere. TGA profiles of nanocomposites are presented in Figure 12. Composite degradation was investigated by measuring weight loss. Thermal degradation can present an upper limit to the service temperature of the composites as much as the possibility of mechanical property loss. We see that nanoparticles contribute to the rise of thermal degradation temperature. The maximum thermal stability has been achieved by introducing 5 wt% nano Al_2O_3, followed by alumina clay mixture and clay composites. The thermal stabilization effect is mostly connected with the high thermal stability of Al_2O_3 nanoparticles and the extent of transfer of thermal energy from major phase to minor phase in a state of improved interface and better dispersion of nanofillers in polymeric matrix.[49-51] For the hybrid sytsem, thermal stability is less than that of the binary Al_2O_3 composite. The main reason behind this is the presence of clay nanoparticles and the less thermally stable very long organic chain on the clay platelets. Another possible explanation for the improvement of thermal stability is the formation of a nanoparticle layer on the surface of the polymer melt, which serves as a barrier preventing further degardation of the underlying polymer.[42] During the thermal degradation of polymer the nano particles will accumulate to the suraface of molten polymer creating a sort of shield that acts as physical protection from heat for the remaining polymer and slowing down the volatilization of the polymer fragments generated by the pyrolysis.[52] Further investigation is currently underway.

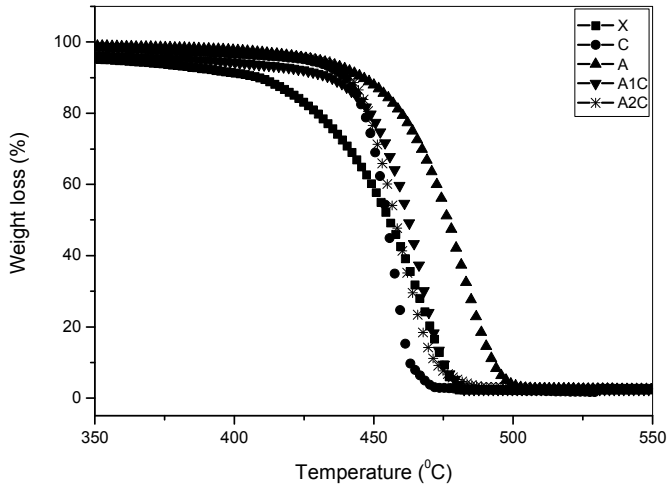

Figure 12: TGA graphs of XLPE (X), XLPE/ Al_2O_3 (A), XLPE/clay (C), XLPE/ Al_2O_3:clay=1:1 (A1C), XLPE/ Al_2O_3:clay=2:1 (A2C)

4. Conclusions

In this work, the morphological, mechanical, dynamical mechanical and thermal characteristics of XLPE/Al_2O_3/clay ternary hybrid systems of Al_2O_3 and clay in 1:1 and 2:1 ratios, binary systems of XLPE/clay and XLPE/Al_2O_3 nanocomposites have been investigated with special reference to the hybrid filler effect and the superior micro structural development in ternary systems. All the nanocomposites exhibit improved mechanics, in which ternary hybrid composite of Al_2O_3 and clay in 1:1 showed highest tensile strength(100 % increase) and Young's modulus (208 % increase), followed by Al_2O_3:clay = 2:1, binary systems of XLPE/Al_2O_3 and XLPE/clay. TEM images support the mechanics by showing the network formation in the ternary hybrid system. This kind of effective networking occurs only in Al_2O_3:clay = 1:1. For Al_2O_3:clay = 2:1 alumina aggregation dominates over hybrid effect in network formation. Theoretical and experimental values of Young's modulus and tensile strength are compared. For A1C (Al_2O_3:clay = 1:1), experimental results show positive hybrid effect, which make it very clear that, in addition to the arithmetic average of the properties of the two fillers, there will be another factor of synergism too *i.e.* filler networks operates in the hybrid system die to the networking associated with self assembly. Nanocomposites are showing higher storage modulus compared to neat XLPE and this is due to the increased stiffness of the material by the incorporation of material with high elastic modulus. Thermal stability of all the nanocomposites are superior to the pristine XLPE and the thermal stabilization effect of nanocomposites is mostly connected with the high thermal stability of nanoparticles and the formation of a protecting layer of naomaterials on polymer surface.

5. References

1. S. P. Thomas, S. Thomas, S. J. Bandyopadhay, *Phys. Chem. C*. 2009, **113**, 97-104
2. W. Cheng, W. Miao, L. Zhang, J. Peng, *Iranian Polymer Journal*, 2011, **20,** 681-687
3. X. Huang, F. Liu, P. Jiang, *IEEE Transactions on Dielectrics and Electrical Insulation*, 2010, **17**, 1697-1704
4. M. S. Nurul, M. Mariatti, *Polym. Bull.* 2013, **70**, 871-884
5. J. Sarlin, K. Immonen, *AIP Conference proceedings*, 2010, **85**, 1255
6. A. Das, K. W. Stockelhuber, S. Rooj, D. Y. Wang, G. Heinrich, *Raw materials and Application*, 2010**,** 296-302
7. J. Li, P. S. Wong, J. K. Kim, *Materials Science and Engneering A***,** 2008, **483-484**, 660-663
8. M. S. Sreekala, J. George, M. G. Kumaran, S. Thomas, *Comp. Sci. Tech*. 2002, **62**, 339
9. J. Fritzsche, H. Lorenz, M. Kluppel, *Macromol. Mater.Eng*. 2009, **294,** 551-560
10. H. F. Kudina, A. I. Burya, *International Scientific Conference*, Gabrovo 19-20 November 2010
11. S. M. Miriyala, Y. S. Kim, L. Liu, J. C. Grunlan, *Macromol. Chem. Phys*. 2008, **209**, 2399-2409
12. D. Maldas, B. V. Kokta, *Polym. Degrad.*, 1991**, 31**, 9
13. M. S. Morsy, S. H. Alsayed, M. Aqel, *Construction and Building Materials*, 2011, **25** , 145–149
14. D. Sun, C. Chu, H. J. Sue, *Chem. Mater*. 2010, **22**, 3773–3778
15. M. F. Uddin, C. T Sun, *Composite Science and Technology***,** 2010, **70**, 223
16. L. Chen, S. Chai, K. Liu, N. Ning, J. Gao, Q. Liu, F. Chen, *ACS Appl. Mater. Interfaces* 2012, **4**, 4398−4404
17. S. M. Zhang, L. Lin, H. Deng, X. Gao, E. Bilotti, T. Peijs, Q. Zhang, Q. Fu, *eXPRESS Polymer Letters,* 2012**, 6,** 159-168
18. K. Litina, A. Miriouni, D. Gournis, M. A. Karakassides, N. Georgiou, E. Klontzas, E. Ttoukas, A. Avgeropoulos, *European Polymer Journal*, 2006, **42**, 2098-2107
19. P. Ma, M. Liu, H. Zhang, S. Wang, R. Wang, K. Wang. Y. Wong, B. Tang, S. Hong, K. Paik, J. Kim, *ACS Applied materials and Interfaces*, 2009, **5**, 1090-1096
20. G. Polizos, V. Tomer, E. Manias, C. A. Randall, *Journal of Applied Physics***,** 2010, **108**, 074117
21. S. N. Leung, M. O. Khan, E. Chan, H. E. Naguib, F. Dawson, V. Adinkrah, L. L. Hayward, *J. Appl. Polym. Sci,* 2013, **10,** 3293-3301
19. D. S. Chaudhary, R. Prasad, R. K. Gupta, S. N. Battacharya, *Thermochimica Acta***,** 2005, **433**, 187-195
20. S. Coiai, D. Prevosto, M. Bertoldo, L. Conzatti, V. Causin, C. Pinzino, E. Passaglia, *Macromolecules*, 2013, **46**,1563-1572
21. J. Ayippadath, S. K. Patel, A. K. Chandra, D. K. Tripathy, *J. Polym. Res*. 2011

22. J. A. Konishi, A. Cakmak, *Polymer*, 2006*,* **47**, 5371
23. L. Bokobza, M. Rahmani, C. Belin, J. Bruneel, N. E. Bounia, *Journal of Polymer Science: Part B: Polymer Physics*, 2008, **46**, 1939-1951
24. P. C. Ma, M. Y. Liu, H. Zhang, S. Q. Wang, R. Wang, K. Wang, Y. K. Wong, B. Z. Tang, S. H. Hong, K. W. Paik, J. K. Kim, *ACS Applied Materials and Interfaces*, 2009, **5**, 1090-1096
25. H. Ismail, A. F. Ramly, N. J. Othman, *Appl. Polym. Sci*. 2012, 1-10
26. J. A. Pople, G. R. Mitchell, S. J. Sutton, A. S. Vaughan, C. K. Chai, *Polymer,* 1999, **40**, 2769-2777
27. J. P. Jose, V. Mhetar, S. Culligan, S. Thomas, *Science of Advanced Materials*, 2013, **5**, 1-13
28. V. M. Litvinov, R. A. Orza, M. Kluppel, M. Duin, *Macromolecules,* 2011, **44**, 4887–4900
29. Y. Rao, J. M. Pochan, *Macromolecules,* 2007*,* **40**, 290-296
30. B. Wunderlich, *Prog. Polym. Sci***.,** 2003, **28**, 383–450
31. T. Selvin, J. Kuruvilla, S. Thomas, *Materials Letters,* 2004, **58**, 281-289
32. C. Schick, A. Wurm, A, Mohammed, *Thermochimica Acta*, 2003, **396***,* 119-132
33. H. Yu, J. Liu, Z. Wang, Z. Jiang, T. Tang, *J. Phys. Chem. C* 2009, **113***,* 13092–1309
34. O. V. D. Berg, W. G. F. Sengers, W. F. Jager, S. J. Picken, M. Wu, *Macromolecules* 2004**, 37***,* 2460-2470
35. A. A. K. Chuk, A. N. Shchegolikhin, V. G. Schvchenko, P. M. Nedorezova, A. N. Klyamkina, M. Aladyshev, *Macromolecules* 2008, **41***,* 3149-3156
36. D. Pista, M. G. Danikas, *NANO:Brief reports and Reviews*, 2011, **6**, 497-508
37. Bhattacharya , M.; Bhowmick, A. K. *J Mater Sci* **2010**, **45**, 6139–6150
38. H. Varghese, S. S. Bhagawan, S. Thomas, *Journal of Applied Polymer Science*, 1999**, 71**, 2335-2364
39. S. Barus, M. Zanetti, M. Lazzari, L. Costa, *Polymer,* 2009, **50**, 2595-2600
40. K. W. Putz, M. J. Palmeri, R. B. Cohn, R. Andrews, L. C. Brinson, *Macromolecules***,** 2008, **41**, 6752-6756
41. M. Idicula, Ph. D. Thesis, M. G. University, India, 2006
42. M. F. Ashby, Y. J. M. Brechet, *Acta Materialia*, 2003, **51**, 5801
43. S. Yang, J. Taha-Tijerina, V. Serrato-Diaz, *Composites: Part B,* 2007**, 38,** 228–235
44. J. Liang, *Materials Sciences and Applications***,** 2010, **1**, 343-349
45. M. Marilda, L. Akcelrud, *J Polym Res* 2008, **15**, 83–88
46. S. H. El-Sabhagh, A. A. Yehia, *Egypt. J. Solids,* 2007, **2,** 157-172
47. M. Bohning, H. Goering, B. Schartel, *Macromolecules,* 2005, **38,** 2764-2774
48. R. Zhang, M. Hummelgard, H. Olin, *Langmuir*, 2010, **26**, 5823-5828
49. S. A. Kumar, H. Yuelong, D. L. Y. Yumei, G. Kumaran, S. Thomas, *Ind. Eng. Chem. Res.* 2008, **47***,* 4898–4904